# ELASMOBRANCH RECTAL GLAND CELL

## Autoradiographic Localization of [$^3$H]Ouabain-Sensitive Na, K-ATPase in Rectal Gland of Dogfish, *Squalus Acanthias*

JILL EVELOFF, KARL J. KARNAKY, JR., PATRICIO SILVA, FRANKLIN H. EPSTEIN, and WILLIAM B. KINTER‡

From the Mount Desert Island Biological Laboratory, Salsbury Cove, Maine 04672; and the Department of Medicine and Thorndike Laboratory, Harvard Medical School and Beth Israel Hospital, Boston, Massachusetts 02215. Dr. Eveloff's present address is the Max-Planck-Institut für Biophysik, Frankfurt, Germany. Dr. Karnaky's present address is the Department of Anatomy, Temple University School of Medicine, Philadelphia, Pennsylvania 19140.

ABSTRACT

Specific binding of radiolabeled inhibitor was employed to localize the Na-pump sites (Na,K-ATPase) in rectal gland epithelium, a NaCl-secreting osmoregulatory tissue which is particularly rich in pump sites. Slices of gland tissue from spiny dogfish were incubated in suitable [$^3$H]ouabain-containing media and then prepared for Na,K-ATPase assay, measurement of radiolabel binding, or quantitative freeze-dry autoradiography at the light microscope level. Gross freezing or drying artifacts were excluded by comparison with additional aldehyde-fixed slices. Characterization experiments demonstrated high-affinity binding which correlated with Na,K-ATPase inhibition and half-saturated at ~5 $\mu$M [$^3$H]ouabain. At this concentration, the normal half-loading time was ~1 h and low-affinity binding to nonspecific sites was negligible. Autoradiographs from both 1- and 4-h incubated slices showed ~85% of the bound [$^3$H]ouabain to be localized within a 1-$\mu$m wide boundary region where the highly infolded basal-lateral cell membranes are closest to the mitochondria. These results establish that most of the enormous Na,K-ATPase activity associated with rectal gland epithelium is in the basal-lateral cell membrane facing interstitial fluid and not in the luminal membrane facing secreted fluid. Moreover, distribution along the basal-lateral membrane appears to be nonuniform with a higher density of enzyme sites close to mitochondria.

KEY WORDS elasmobranch rectal gland · [$^3$H]ouabain autoradiography · Na pump localization · NaCl-secreting epithelium · ouabain-sensitive Na,K-ATPase

‡ Deceased 6 October 1978.

The elasmobranch rectal gland, as found in the spiny dogfish, *Squalus acanthias*, is an osmoregulatory organ which secretes a fluid with a high concentration of NaCl, higher than seawater and almost twice as high as plasma (3). When perfused



J. CELL BIOLOGY © The Rockefeller University Press · 0021-9525/79/10/0016/17 $1.00
Volume 83 October 1979 16–32

in vitro, this gland exhibits active secretory transport of salt which is modulated by an adenylate cyclase-cyclic (c) AMP system, because the addition of dibutyryl cAMP or theophylline to the perfusate immediately increased the level of NaCl excretion severalfold (35). In addition, salt secretion by the rectal gland is linked to a very high concentration of the ouabain-sensitive, Na- and K-dependent ATPase (Na,K-ATPase); in fact, the dogfish gland is one of the richest known sources of this membrane-bound enzyme (1, 15). Other salt-secreting osmoregulatory organs also exhibit high Na,K-ATPase activities which can be correlated with transepithelial NaCl transport by the gland or tissue. For example, the salt-stressed avian nasal gland or euryhaline teleost gill responds by increases in enzyme activity and NaCl excretion (13, 17, 23). Moreover, Na,K-ATPase has been localized primarily to the basal-lateral membranes of the secretory cells in both duck nasal gland and killifish gill (9, 10, 16). Because the role of this membrane-bound enzyme is believed to be active transport of Na out of the cell with a concomitant transfer of K inwards (15, 27), basal-laterally located Na,K-ATPase suggests that Na is pumped toward the blood side of the secreting cell, i.e., the Na pump appears to be oriented in the wrong direction for NaCl elimination from the salt-stressed animal.

In view of the above, it was clearly important to determine whether Na,K-ATPase is also located basal laterally in the cells of the salt-secreting rectal gland. The only previous attempt to localize this enzyme employed Sr-capture Pb-substitution cytochemistry (14). In the present study, we have employed a different approach: quantitative autoradiography of bound [$^3$H]ouabain at the light microscope level. Ouabain sensitivity is a part of the general definition for Na,K-ATPase activity, and this method has proven to be highly specific for Na,K-ATPase sites in many epithelial tissues (10, 16, 21, 22, 24–26, 28, 31, 32). The results presented here establish that the basal-lateral localization of the Na,K-ATPase extends to the epithelial cells of the dogfish rectal gland. Moreover, we report for the first time a nonuniform enzyme distribution along the basal-lateral membrane, i.e., Na,K-ATPase restricted to portions close to mitochondria. Finally, modulation of rectal gland secretion by the cAMP system does not appear to involve changes in Na,K-ATPase activity.

## MATERIALS AND METHODS

### *Animal and Slice Preparation*

Spiny dogfish, *S. acanthias*, weighing between 3 and 5 kg, were taken by hook and line from Frenchman's Bay at Mount Desert Island, Maine, maintained in marine live cars, and used for study within 2 d of capture. After the dogfish was killed by segmentally severing the spinal cord, the rectal gland was rapidly removed and placed in ice-cold dogfish Na-Ringer's solution (composition in mM: NaCl, 280; KCl, 6; $CaCl_2$, 2.5; $MgCl_2$, 3; urea, 350; glucose, 5; $Na_2SO_4$, 0.5; $NaH_2PO_4$, 1; $NaHCO_3$, 8; pH 7.6 at room temperature). In preparation for slicing, the rectal gland was cut open and the central canal removed. The outer surface of a roughly 0.5-cm$^3$ cube of the gland, which is covered with a tough connective tissue capsule, was glued with Locktite tissue adhesive (Locktite Corp., Nevington, Conn.) to an aluminum chuck. The tissue was covered with warm 3% agar-agar in Na-Ringer's to provide support during slicing, placed in ice-cooled Na-Ringer's, and 150- to 200-$\mu$m slices were cut with a Vibratome sectioning system (Oxford Laboratories Inc., Foster City, Calif.).

### *Ouabain Binding in Rectal Gland Slices*

To determine the incubation period necessary for steady-state or saturation binding, several rectal gland slices, representing ~15 mg of tissue, were incubated at 15°C for varying time periods in 2 ml of one of the following media: (*a*) Na-Ringer's; (*b*) Na-Ringer's plus 0.05 mM dibutyryl cAMP ($N^6$, $O^{2'}$-dibutyryl adenosine 3′;5′-cyclic monophosphoric acid, monosodium salt) and 0.25 mM theophylline; (*c*) high K-Ringer's, in which KCl was increased to 65 mM and NaCl was decreased to 221 mM; or (*d*) high K-Ringer's plus 0.05 mM dibutyryl cAMP and 0.25 mM theophylline. Aeration was maintained by moderate shaking of unstoppered incubation vessels. [$^3$H]Ouabain (12 Ci/mmol) plus unlabeled ouabain was added to the incubation media to achieve a final concentration of 5 $\mu$M (1 $\mu$Ci/ml for binding studies; 60 $\mu$Ci/ml for autoradiography). To study the effects of increasing ouabain concentration on ouabain binding, unlabeled ouabain was added to the incubation media up to final concentrations of 1,000 $\mu$M. To determine the efficacy of postincubation washing and the size of the extracellular space, [$^{14}$C]inulin was added to the incubation media at 10 mg/100 ml (3 mCi/g). At the end of the incubation period, the slices were washed twice in 6 ml of Ringer's of the same composition as the original incubation medium, minus the ouabain and inulin, for a total of 30 min. Slices were then removed from the wash fluid, weighed, and solubilized in counting vials with 1 ml of NCS tissue solubilizer (Amersham Corp., Arlington Heights, Ill.) plus 0.1 ml $H_2O$. For estimation of extracellular space, [$^{14}$C]inulin was also measured in unwashed slices after incubation. Conven-

tional liquid scintillation counting techniques with external standard ratio quench correction were used to measure the $^{3}H$ and $^{14}C$ content of tissue and fluid samples. Radiolabeled compounds were obtained from New England Nuclear (Boston, Mass.), and unlabeled compounds such as ouabain, dibutyryl cAMP, and ATP were obtained from Sigma Chemical Co. (St. Louis, Mo.).

### *Na,K-ATPase Assay*

The effect of ouabain, 5–1,000 $\mu$M, on Na,K-ATPase activity was determined in vitro in rectal gland slices. The effect of dibutyryl cAMP, 0.05 mM, and theophylline, 0.25 mM, on Na,K-ATPase was also investigated in slices. In addition, Na,K-ATPase activity was measured in fresh rectal gland tissue with dibutyryl cAMP concentrations varying from $10^{-10}$ to $10^{-3}$ M and/or theophylline of 0.25 mM in the assay medium.

In the ouabain experiments, slices were incubated at 15°C for 4 h, washed in Ringer's for 30 min, and homogenized in 0.25 M sucrose and 5 mM EDTA in a 1:45 ratio (wt/vol). The homogenate was shell frozen in a vial using dry ice and ethanol, freeze dried at −20°C for 15 h, and stored at −20°C until the assay was performed, usually within 5 wk. For the enzyme assay, freeze-dried homogenate was taken up in 2 ml of homogenizing solution, and Na,K-ATPase activity was measured as the difference in inorganic phosphate ($P_i$) liberated from ATP in the presence and in the absence of 1,000 $\mu$M ouabain. The assay medium consisted of 100 mM NaCl, 20 mM KCl, 6 mM MgCl, 10 mM imidazole, and 6 mM ATP. The temperature of incubation was 37°C and the samples were incubated for 15 min. The rest of the enzyme assay was carried out as previously described (30). The results were expressed as micromoles of $P_i$ liberated per milligram of protein per hour. Bonting (1) originally noted that lyophilization releases as much Na,K-ATPase activity from tissue homogenates as deoxycholate treatment and offers the advantage that they can be stored at low temperature for several months with no loss of enzyme activity. This fact was confirmed here (Results).

Rectal gland slices incubated with dibutyryl cAMP and theophylline for 4 h at 15°C were homogenized in 0.25 M sucrose, 20 mM imidazole, 6 mM EDTA, and 1% (wt/vol) deoxycholate. The homogenates were then assayed as described above for the ouabain experiments. Finally, fresh rectal gland tissue was homogenized with deoxycholate and assayed with varying concentrations of dibutyryl cAMP and/or theophylline in the assay medium. Otherwise, the assay was performed as above.

### *Morphology and Autoradiography*

For comparison of aldehyde-fixed and freeze-dried morphology, rectal gland slices from several fish were examined after incubation for 1 or 4 h in Na-Ringer's or Na-Ringer's plus 5 $\mu$M ouabain. Pieces of unincubated, i.e. fresh, gland tissue were also fixed in aldehyde. Final [$^{3}H$]ouabain autoradiographs were prepared from freeze-dried slices representing two fish. For aldehyde-fixed morphology, fixation was carried out with 6% glutaraldehyde in cacodylate buffer followed by post-fixation in osmium tetroxide and embedding in Epon according to the procedures of Karnaky et al. (16). For freeze-dry morphology and autoradiography, the slices were spread on aluminum foil, frozen in liquid propane at −185°C, stored in liquid nitrogen, and then freeze dried according to the method of Karnaky et al. (16). The dried slices were fixed overnight in osmium tetroxide vapor, cut into about five small pieces, and embedded in silicone-impregnated epoxy resin, Spurr Low-Viscosity (Polysciences, Inc., Warrington, Pa.). Sections for the electron microscope (500–800 Å) were cut over water with a diamond knife, stained for 20 min with 2% aqueous uranyl acetate, pH 5.0, washed in distilled water, and counterstained for 5 min with lead citrate. These sections were examined with either a Philips 300 or a Hitachi HU-11C electron microscope. Light microscope sections (0.8–1.2 $\mu$m) were cut over water using glass knives and, when not used for autoradiography, these plastic-embedded sections were stained directly with methylene blue and Azure II. Both directly stained sections and autoradiographs were examined and photographed with a light microscope equipped with Zeiss phase-contrast optics. To determine the relative area occupied by each region of the rectal gland cell, photomicrographs of both aldehyde-fixed tubules and directly stained, freeze-dried tubules were enlarged, cut up with scissors, and the weight of each region was expressed as a percent of the whole tubular epithelium. All final freeze-dry morphology and autoradiography reported in this study represent tubules showing minimal freezing artifacts.

For autoradiography, initially unstained light microscope sections were coated with a 2-$\mu$m layer of NTB-2 emulsion (Eastman Kodak Co., Rochester, N.Y.) and processed according to the procedure of Karnaky et al. (16). Autoradiographic exposure times generally ranged from 3 to 33 d and, following development of the silver grains in the exposed emulsion, the underlying plastic-embedded tissue was lightly stained with methylene blue and Azure II. Evaluation for technical artifacts revealed neither gross leaching of [$^{3}H$]ouabain into the embedding plastic or the emulsion coat, nor any tissue-induced chemography, positive (chemical fogging) or negative (latent-image fading). Moreover, reciprocity between grain density and exposure time was observed over rectal gland cells, confirming the absence of latent-image fading and indicating that the emulsion was not saturated at densities employed for grain counting (<700 grains/1,000 $\mu m^2$). Counting was performed under the phase-contrast optics so that all individual grains over a given area of tubular epithelium could be accurately assigned to specific cell regions. An ocular grid, equivalent to 4 $\mu$m on a side at the magnification used, served both to help assign grains to the 1-$\mu$m wide membrane-mitochondrial boundary region and to measure the total area

of tubular epithelium over which grains were counted. From this total area, in square micrometers, and the relative areas of each cell region, in percent, regional grain densities were calculated and, after subtracting the background density measured over adjacent plastic alone, were expressed as grains/1,000 $\mu m^2$ per d autoradiographic exposure. Each total count for a particular tissue section consisted of 200–600 grains, which in the case of the grain-rich boundary region should give a methodological coefficient of variability of within 20% of the absolute density values over different sections (16). Besides random variation in autoradiographic density from section to section, a systematic lowering of density can occur over grain-rich bands because of resolution limitation with the $^3$H-label. In tests with earlier versions of the present autoradiographic technique, the resolution error for a 1-$\mu m$ wide band was less than the random density variation (33, 34). Thus, for the present 1-$\mu m$ boundary region, the overall accuracy for density values was estimated to be ±25%. Finally, grain density was converted to ouabain content, in picomoles per milligram tissue, using the autoradiographs of [$^3$H]ouabain standards which were originally prepared for this purpose by Karnaky et al. (16).

## RESULTS

### *Ouabain Binding and Na,K-ATPase Activity in Slices*

For autoradiographic localization of bound [$^3$H]ouabain to be meaningful, it must be established that this inhibitor is specifically bound to rectal gland Na, K-ATPase under the incubation conditions used. The effect of ouabain concentration on binding to rectal gland slices at 15°C is shown in Fig. 1. Increasing the concentration in Na-Ringer's medium decreased the relative tissue content of bound ouabain, as reflected by 4-h tissue/medium ratios, and, thus, indicated saturability of the binding reaction. At the lower ouabain concentrations, 5 and 25 $\mu M$, inhibition by high K-Ringer's was apparent. Furthermore, as shown in Fig. 2, Na,K-ATPase activity can be correlated with the ouabain binding in slices incubated in increasing glycoside concentrations for 4 h. Enzyme inhibition parallelled ouabain binding until nearly total inhibition was achieved with 100 $\mu M$ ouabain in the Na-Ringer's incubation medium. Additional low-affinity binding at still higher concentrations most likely represents nonspecific binding to other tissue sites that are not involved in Na,K-ATPase inhibition. Based on the data in Fig. 2, the half-saturation concentration of free glycoside at which half the specific rectal gland sites are filled (Ki) corresponds to ~5 $\mu m$ ouabain.

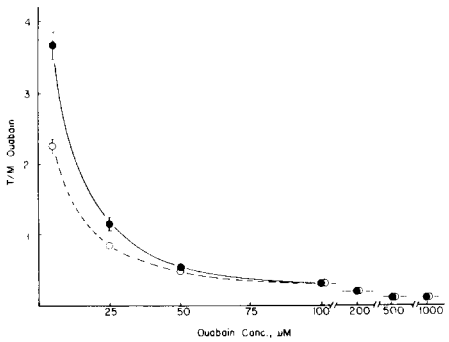


FIGURE 1 Ouabain binding in dogfish rectal gland slices as a function of ouabain concentration in incubation media. Binding is expressed as the tissue content (T in pmol ouabain/mg) divided by the medium concentration (M in $\mu$mol ouabain/liter). The medium was either Na-Ringer's (solid circles) or high K-Ringer's (open circles) with 6 or 65 mM K, respectively. The 200-$\mu m$ slices were incubated for 4 h at 15°C in a given ouabain concentration and then washed for 30 min in the corresponding ouabain-free medium. Individual values are means, with ± SE bars when the latter are larger than the symbols ($n$ = 4 fish).

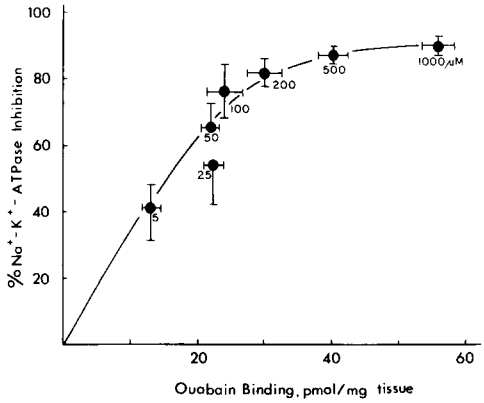


FIGURE 2 Correlation between inhibition of Na,K-ATPase activity and ouabain binding in rectal gland slices. All data are for 200-$\mu m$ slices incubated 4 h at 15°C in Na-Ringer's with ouabain concentrations ranging from 5 to 1,000 $\mu M$ (given numerically next to each symbol) and then washed 30 min in ouabain-free Na-Ringer's. Paired slices from the same fish were assayed, respectively, for ouabain and for Na,K-ATPase (freeze-dry method). Individual values are means with ± SE bars ($n$ = 4 fish). The control or uninhibited activity value for slices incubated without ouabain was 48.0 ± 12.3 $\mu$mol $P_i$/mg protein per h.

Binding-rate experiments with this concentration in the incubation media are shown in Fig. 3. In Na-Ringer's, ouabain binding by rectal gland

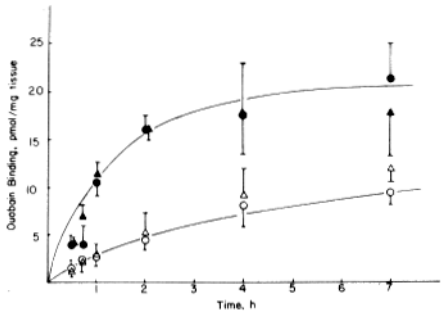


FIGURE 3 Ouabain binding in rectal gland slices as a function of incubation time in 5 $\mu$M ouabain. The following incubation media were tested: Na-Ringer's (solid circles), high K-Ringer's (open circles), and 0.05 mM dibutyryl cAMP plus 0.25 mM theophylline in the former (solid triangles) and the latter (open triangles). All data are for 200-$\mu$m slices incubated at 15°C for a given time and then washed in the corresponding ouabain-free medium for 30 min. Individual values are means with ± SE bars ($n$ = 4–6 fish, generally). Curves are based on least squares lines in Fig. 4.

TABLE I

*Inulin Uptake into Rectal Gland Slices Incubated at 15°C in Na-Ringer's*

| Incubation time | Inulin distribution space* |
|---|---|
| *min* | *% tissue volume* |
| 30 | 40.6 ± 3.5 |
| 100 | 43.7 ± 5.2 |
| 130 | 39.8 ± 4.1 |
| after 30 min washout | 7.2 ± 0.5 |

* Mean ± SE ($n$ = 3–5 fish) assuming unit tissue density.

slices was only approaching a steady state after 2 h of incubation at 15°C. In contrast, uptake of the extracellular marker inulin had reached a steady state by 30 min, the shortest time period tested (Table I). Fig. 4 shows double reciprocal plots of data from Fig. 3. With 5 $\mu$M ouabain in Na-Ringer's, the half-loading time, estimated from the x-axis intercept, was 1.25 h and the steady-state binding, estimated from the y-axis intercept, was 26.7 pmol ouabain/mg tissue. Thus, the rate of ouabain binding by dogfish rectal gland slices at 15°C appears relatively slow when compared to duck nasal gland slices, where the half-loading time from 4.4 $\mu$M ouabain at 37°C was only 3 min (10). High K concentrations, which are known to slow the rate of ouabain binding by Na,K-ATPase (27), are regularly used to establish specificity for autoradiographic studies (10). With rectal gland slices (Fig. 3), 65 mM K-Ringer's markedly slowed the binding rate in 5 $\mu$M ouabain. Estimates from the double reciprocal plot (Fig. 4) show a highly significant ($P < 0.01$) increase in the half-loading time to 5.50 h, but a nonsignificant ($P < 0.05$) reduction in the steady-state binding to 17.4 pmol ouabain/mg tissue. Because 5 $\mu$M [$^3$H]ouabain also approximates the Ki and permits establishment of suitable levels of tissue radioactivity, this concentration was selected for rectal gland slice autoradiography.

Salt secretion by the isolated, perfused rectal gland is maximally stimulated by dibutyryl cAMP plus theophylline (35) and, because the rate of Na pumping has been correlated with the rate of ouabain binding in some tissues (4), the effect of 0.05 mM dibutyryl cAMP plus 0.25 mM theophylline on ouabain binding was examined in rectal gland slices. There was, however, no significant effect ($P > 0.05$) on ouabain binding in either Na-Ringer's or high K-Ringer's (Fig. 3). Likewise, there was no effect on the Na,K-ATPase activity in slices incubated for 4 h in Na-Ringer's with the

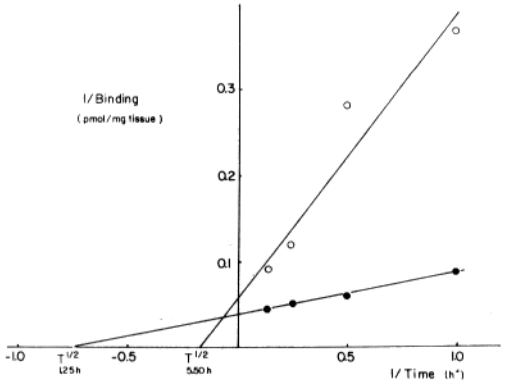


FIGURE 4 Double reciprocal plots of binding-rate data from Fig. 3. Because ouabain binding was the same with and without dibutyryl cAMP plus theophylline, means were combined for Na-Ringer's (solid circles) and for high K-Ringer's (open circles) and fitted to least squares lines. Only the 1- to 7-h data were used, because, particularly with Na-Ringer's, restricted diffusion within slices may have erroneously limited the binding at incubation times shorter than 1 h (Fig. 3). The binding of ouabain to the Na,K-ATPase molecule is bimolecular and therefore, strictly, follows second order kinetics, but because <3% of the ouabain present in the incubation medium was bound, the concentration is effectively constant throughout the incubation period and the binding reaction approximates first order kinetics. Thus, the kinetic constants determined from the double reciprocal plots are empirically accurate (10).

above combination of dibutyryl cAMP plus theophylline (data not shown). Moreover, as shown in Table II, assaying homogenates of fresh glands in the presence of these stimulatory compounds did not alter the Na,K-ATPase activity. Finally, it should be noted that the actual Na,K-ATPase activities for fresh rectal glands (Table II) and incubated slices (Fig. 2, legend) are very high, i.e., ~40 μmol $P_i$/mg protein per h, and agree well with activities reported originally by Bonting (1) and recently by Silva et al. (30).

### *Comparison of Aldehyde-fixed and Freeze-dried Morphology*

The rectal gland of the spiny dogfish has been described in detail by Bulger (2), and only pertinent morphology will be considered here. Briefly, the gland consists of simple and branched tubules which join a central collecting canal that ultimately empties into the postvalvular intestine. Micrographs of aldehyde-fixed tissue taken directly from the animal, i.e. without incubation, are shown in Figs. 5 and 6. The tubules are closely packed in a matrix of connective tissue and vascular elements. The tubular epithelium is comprised of a single layer of large pyramidal to columnar cells, the apices of which face onto a lumen which runs into the central canal. Incubation of rectal gland slices for 4 h in Na-Ringer's (Fig. 7) or Na-Ringer's containing 5 μM ouabain (Fig. 8) produced only minor changes in the gross morphological appearance of aldehyde-fixed tubules. In addition to some swelling of the connective tissue matrix between tubules, the light bands, representing basal-lateral spaces with membrane infoldings, appear slightly enlarged. Area measurements from photomicrographs such as Figs. 6–8 confirm that incubation with or without 5 μM ouabain produced only minimal cell changes at the light microscope level (Table III). Electron micrographs of incubated, aldehyde-fixed tubules (Figs. 9 and 10) illustrate the remarkable complexity of the secretory cell. The basal-lateral plasma membrane is highly infolded over thin plication of cytoplasm, and the resulting extracellular fluid channels extend both into the interior of the cell and almost to the apical border. These folded "membrane" regions are extremely tortuous and extensively interdigitated with adjacent cells. The apical border, in contrast, has a few blunt microvilli and attaches to adjacent cells by typical junctional complexes. The second striking feature of the rectal gland cell is the large number of mitochondria which are closely packed into dense clusters with minimal cytoplasm. In effect, these "mitochondrial" regions and the intervening membrane regions constitute all of the cell except for the centrally located "nuclear" region and a narrow zone comprising the "apical" region.

Although bound ouabain disappears totally from tissue prepared by conventional histological methods such as present aldehyde fixation, rapid freezing followed by freeze drying is suitable for autoradiographic localization of the binding sites (32). Rectal gland slices proved particularly difficult to freeze, perhaps because of the high osmolarity and/or urea content of tissue fluids, and only the most rapidly frozen outer portions were usable. Electron micrographs from the outer portions of freeze-dried, rectal gland slices (Figs. 11 and 12) demonstrate that the major ultrastructural features of the secretory cell are still identifiable in spite of the ice crystal formation and cryosmotic distortion which is known to occur during initial freezing (19). For example, basal-lateral membrane regions appear as lacy networks of infoldings which are interspersed among mitochondrial regions containing dense, shrunken mitochondria (Fig. 12). Some cryosmotic shrinkage is also exhibited by nuclei (Fig. 11). At the light microscope level used for autoradiography (Fig. 14), freezing artifacts are less obvious due to lower magnification and thicker sections. Moreover, area measurements from photomicrographs such as Fig. 14 (Table III) do not differ significantly ($P > 0.05$) from those for aldehyde-fixed slices incubated under similar conditions. For present freeze-dry autoradiography, the important morphological find-

TABLE II

*Na, K-ATPase Activity in Fresh Rectal Gland Homogenate Assayed with 0.25 mM Theophylline plus Decade Concentrations of Dibutyryl cAMP*

| Assay medium: cAMP concentration | | Na,K-ATPase activity* |
|---|---|---|
| *M* | | *μmol Pi/mg protein × h* |
| Control | | 39.4 ± 2.6 |
| Theophylline, alone | | 38.8 ± 2.0 |
| Theophylline, plus: | $10^{-10}$ | 37.9 ± 3.5 |
| | $10^{-6}$ | 42.7 ± 2.9 |
| | $10^{-4}$ | 39.9 ± 4.9 |
| | $10^{-3}$ | 40.6 ± 5.0 |

* Mean ± SE ($n$ = 3–5 fish) by deoxycholate method. Values for the other cAMP concentrations in decade steps between $10^{-10}$ and $10^{-3}$ M (not shown), likewise, did not differ significantly from control ($P > 0.05$).

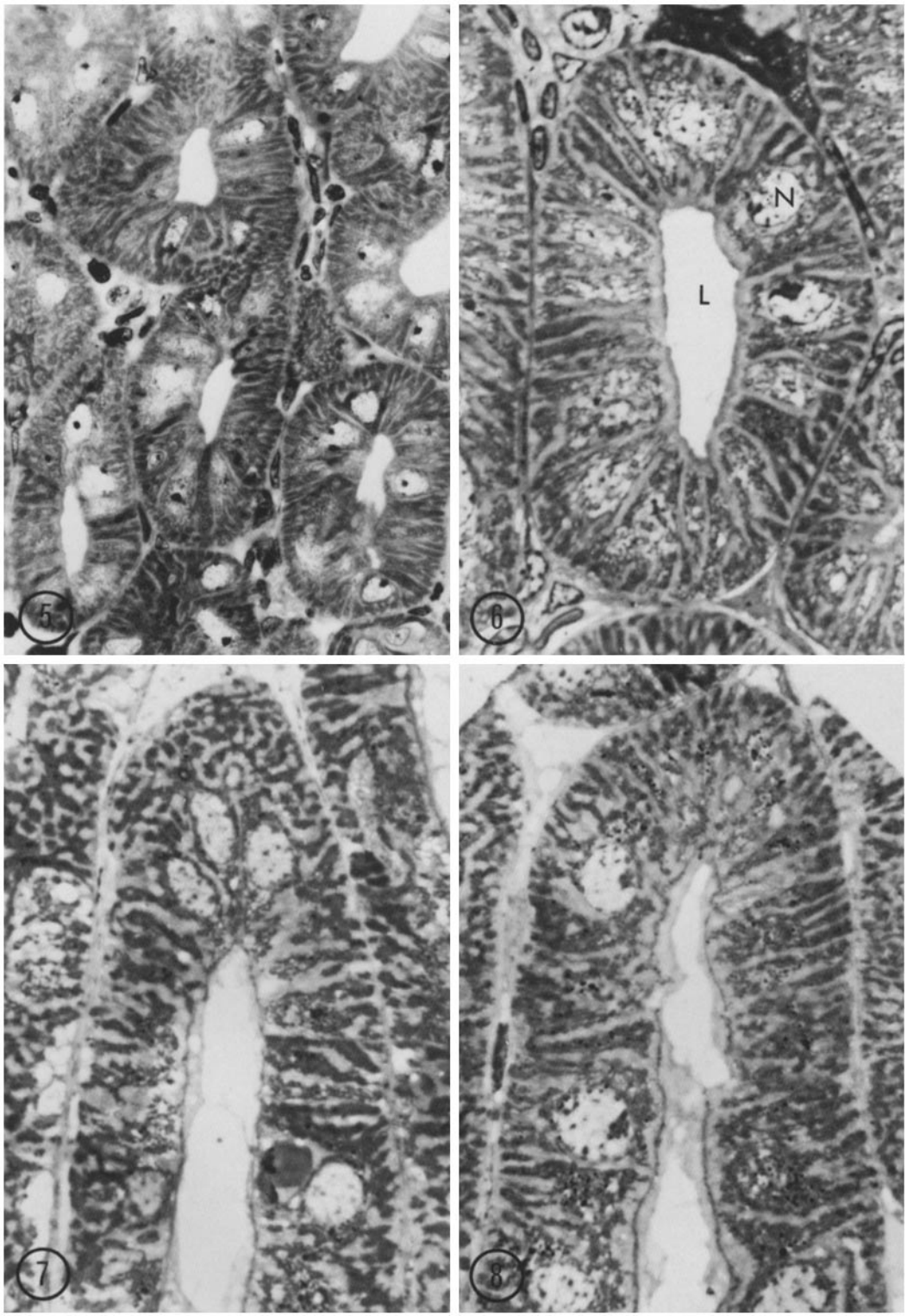
N
L
5
6
7
8

TABLE III

*Comparison of the Relative (%) Areas Occupied by Primary Cell Regions in Aldehyde-Fixed and Freeze-Dried Rectal Gland Tissue**

| | Aldehyde-fixed‡ | | | Freeze-dried§ | |
|---|---|---|---|---|---|
| | | Slices incubated 4 h in | | Slices incubated in ouabain for | |
| Cell region | Fresh tissue | Na-Ringer's | Ouabain | 1 h | 4 h |
| | | *% total cell* | | | |
| Apical | 2.0 ± 0.4 | 1.5 ± 0.4 | 1.7 ± 0.4 | 2.7 ± 0.4 | 2.5 ± 0.2 |
| Nuclear | 6.3 ± 1.5 | 7.0 ± 1.1 | 6.5 ± 1.6 | 8.6 ± 1.2‖ | 4.9 ± 1.1‖ |
| Membrane (total) | 33.3 ± 0.7¶ | 42.3 ± 0.8 | 42.8 ± 1.3 | 39.5 ± 1.0 | 40.8 ± 2.3 |
| Mitochondrial (total) | 58.4 ± 0.9¶ | 49.2 ± 0.5 | 49.1 ± 0.9 | 49.2 ± 0.8 | 52.3 ± 1.9 |

* Slices were incubated at 15°C in Na-Ringer's with or without 5 μM ouabain for the number of hours indicated and then washed in Na-Ringer's alone for 30 min.

‡ Mean ± SE ($n$ = 4 sections representing two fish).

§ Mean ± SE ($n$ = 10 and 3 sections representing two and one fish, respectively, for 1- and 4-h incubation).

‖ Includes shrinkage clefts present around some nuclei; cleft area too small for separate measurement.

¶ Significantly ($P < 0.05$) different from aldehyde-fixed incubated slices.

ings are that the primary regions of the rectal cell are basically intact, even at the ultrastructural level, and that these regions occupy the same relative areas as in aldehyde-fixed slices.

In the course of autoradiographic grain density analysis, the boundary between the two largest cell regions, total mitochondrial and total basal-lateral membrane (Table III), assumed particular interest, and a 1-μm wide boundary region was defined as shown in Fig. 13. The relative area of this "membrane-mitochondrial boundary" region and the areas of the remaining "central membrane" and "central mitochondrial" regions are given in Table IV. The choice of 1 μm as the width of the boundary region was based on the irregularity of the actual interface between membranes and mitochondria seen at the ultrastructural level (Figs. 11 and 12) and the limitation of autoradiographic resolution reported for the present methodology at the light microscope level. Furthermore, this choice conveniently separated the tubular epithelium into three major regions which were roughly

FIGURE 5 Fresh dogfish rectal gland with aldehyde fixation. The closely packed tubules (cut in cross-section) exhibit open lumens and small amounts of surrounding connective and vascular tissue. A single tubule is shown at higher magnification in Fig. 6. Moderately stained, 1-μm plastic section of unincubated, aldehyde-fixed tissue photographed with bright-field optics. × 350.

FIGURE 6 Fresh rectal gland tubule with aldehyde fixation. Seen in cross-section, the tubular epithelium consists of pyramidal to columnar cells with centrally located nuclei ($N$) and an apical zone (light appearing) bordering the open lumen ($L$). The remainder of the cells consist principally of mitochondrial clusters (very dark patches or strips) separated by infolded basal-lateral membranes (narrow light bands). Moderately stained, 1-μm plastic section of unincubated, aldehyde-fixed tissue photographed with phase-contrast optics. × 1,000.

FIGURE 7 Ringer's-incubated tubule with aldehyde fixation. Seen in slightly oblique section, the only obvious morphological difference from the fresh tubule (Fig. 6) is some swelling of the surrounding connective tissue and the basal-lateral membrane bands (Table III). Section of rectal gland slice incubated 4 h at 15°C in Na-Ringer's: processed and photographed as in Fig. 6. × 1,000.

FIGURE 8 Ouabain-incubated tubule with aldehyde fixation. Seen in slightly oblique section, there is no obvious morphological difference from the Ringer's-incubated tubule (Fig. 7). Section of rectal gland slice incubated 4 h at 15°C in Na-Ringer's containing 5 μM ouabain; processed and photographed as in Fig. 6. × 1,000.

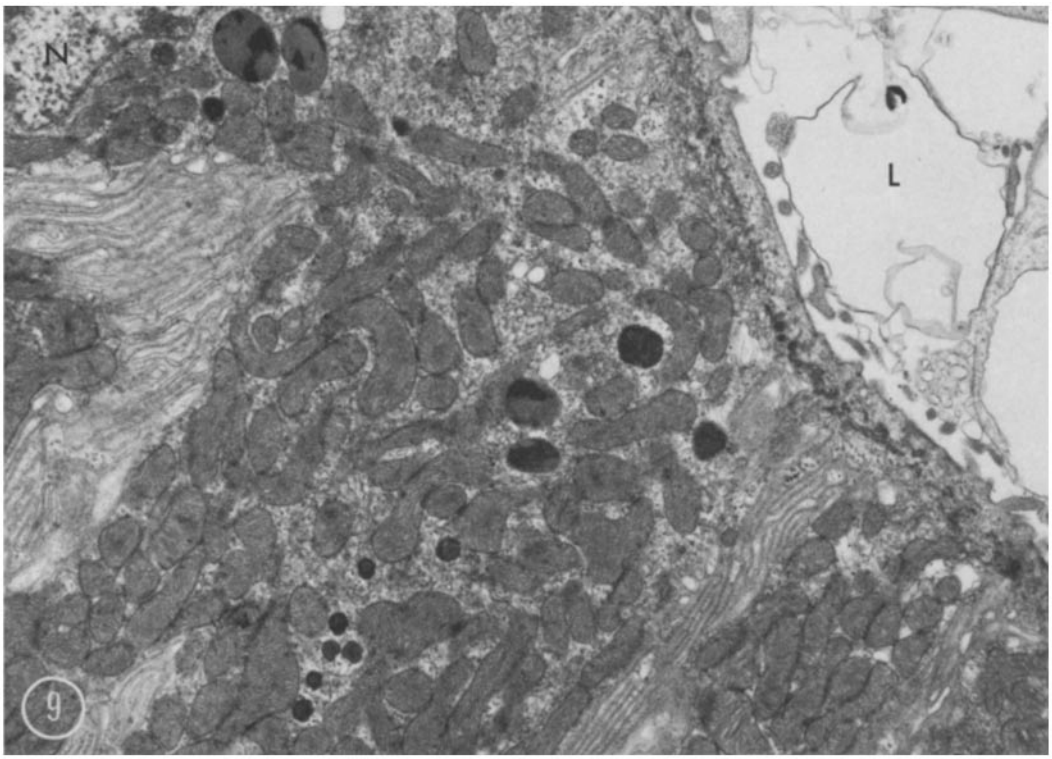


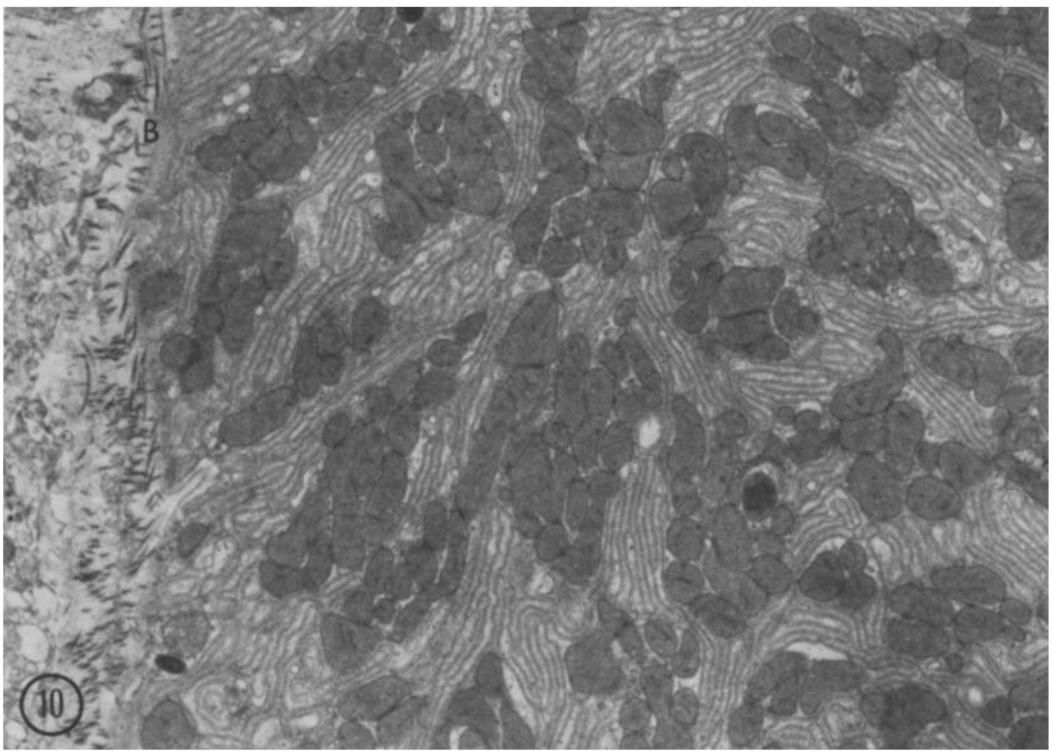


FIGURES 9 and 10 Electron micrographs of incubated tubular cells with aldehyde fixation. The apical end of the cell, which borders the tubular lumen (*L*, Fig. 9), is relatively undifferentiated with a few blunt microvilli, a narrow apical compartment, and typical junctional complexes connecting to adjacent cells. The infoldings of basal-lateral membrane and the associated mitochondrial clusters extend from the membrane-free apical compartment, by the nucleus (*N*, Fig. 9) to the basal lamina (*B*, Fig. 10). Fig. 10 represents an oblique cut through the basal end of several cells and demonstrates the intimate association between closely packed mitochondrial clusters and extensively infolded basal-lateral membranes. Thin sections of rectal gland slices incubated 4 h at 15°C in Na-Ringer's, aldehyde fixed, and processed for electron microscopy. × 10,000.

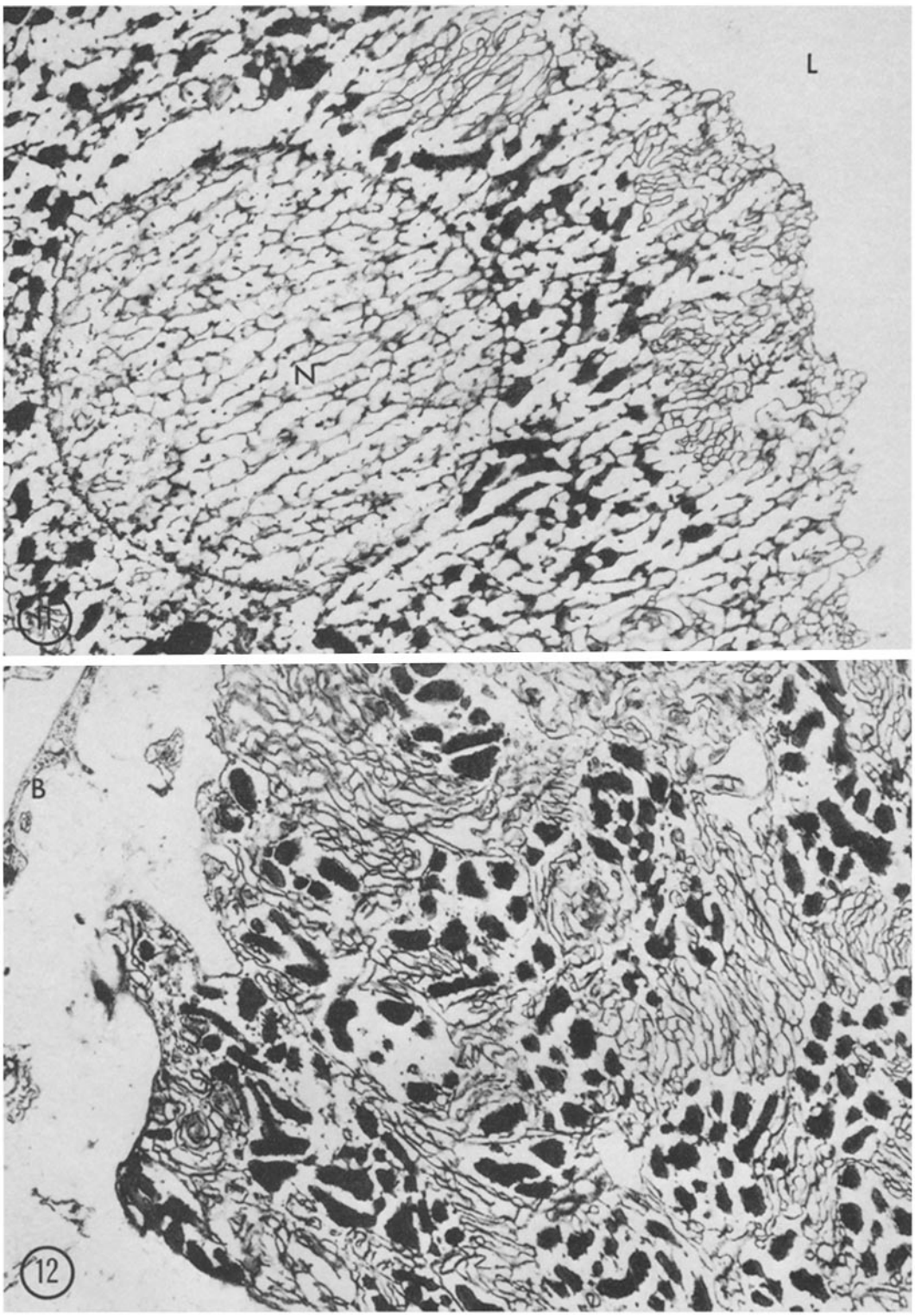


FIGURES 11 and 12 Electron micrographs of incubated tubular cells after freezing and freeze drying. To facilitate comparison with aldehyde-fixed morphology (Figs. 9 and 10), the orientation is similar with a tubular lumen (*L*) in Fig. 11 and some basal lamina (*B*) in Fig. 12. Cryosmotic shrinkage of intracellular organelles is evidenced by the open cleft above the nucleus (*N*, Fig. 11) and the extreme condensation of the mitochondria (solid black spots). More important, the infoldings of basal-lateral membrane (lacy networks) have remained largely intact and in position relative to mitochondrial clusters. The freeze-dried tissue illustrated here is some of that actually used for light microscope-level autoradiography (Figs. 14–17). Thin sections of a rectal gland slice incubated 1 h at 15°C in Na-Ringer's with 5 $\mu$M ouabain, rapidly frozen, freeze dried, and processed for electron microscopy. × 10,000.

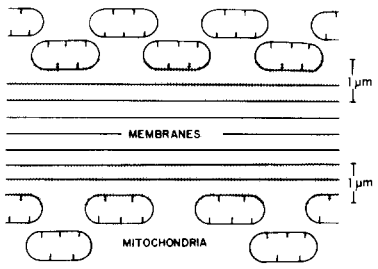


FIGURE 13 Schema defining a 1-μm wide, boundary region (stippled bands) at the interfaces between basal-lateral membranes and mitochondria. The remaining (nonstippled) areas represent central membrane and central mitochondrial regions. For orientation of this schema see the corresponding rectangle in Fig. 14. For autoradiographic grain density measurement (Materials and Methods), all grains lying at least in part over the defined 1-μm band were assigned to the boundary region. As viewed in the phase-contrast counting microscope (Materials and Methods), individual grain diameters averaged 0.5 μm.

equal in area and also remarkably consistent from tubule to tubule, as shown by the low SE values in Table IV. The small apical and nuclear regions, together, occupied only 10% of the cell.

### *Autoradiographic Localization of Ouabain Binding*

Rapid freeze, freeze-dry plastic-section autoradiography provides a direct means for visualizing the tissue distribution of bound [$^3$H]ouabain at the light microscope level. The autoradiographs in Figs. 15–17 show cross sections of the same rectal gland tubule with increasing autoradiographic exposure times of 3, 9, and 33 d, respectively. These sections are representative of slices incubated for 1 h in 5 μM ouabain followed by 30 min in ouabain-free Na-Ringer's. The autoradiographic grains, which appear as black dots overlying the tissue sections, increase in number with longer exposure but consistently exhibit the same distribution pattern. Small numbers of background grains, unrelated to the distribution of bound [$^3$H] ouabain, are seen over the tubular lumen and other large noncellular spaces. Only slightly more grains are seen over either connective tissue or the following regions of the tubular epithelium: cell nucleus, narrow apical zone (which includes the luminal membrane), and central portion of the darkly stained mitochondrial clusters. In contrast, most of the autoradiographic grains appear to be associated with the lightly stained basal-lateral membranes. Closer visual inspection, however, indicates a nonuniform distribution, with most of the grains at any given exposure (Figs. 15–17) being located over the membrane-mitochondrial boundary and only a few over the central membrane region (Fig. 13). Furthermore, this unique distribution with most grains being over the boundary persists even when ouabain binding is approaching steady state in 4-h incubated slices (Fig. 18).

TABLE IV

*Autoradiographic Localization of Bound [$^3$H]Ouabain in Dogfish Rectal Gland Slices after 1 and 4 h of Incubation**

| Cell region | Area‡ | Grain density§ | |
|---|---|---|---|
| | | 1 h | 4 h |
| | *% total cell* | *grains/1,000 μm²/d exposure* | |
| Apical | 2.7 ± 0.3 | 10.6 ± 2.2‖ | 16.9 ± 2.0 |
| Nuclear | 7.7 ± 1.1 | 0.8 ± 0.4 | 1.1 ± 1.4 |
| Membrane¶ | 21.7 ± 1.0 | 4.0 ± 0.9‖ | 5.9 ± 3.1 |
| Mitochondrial¶ | 31.8 ± 0.5 | 0.5 ± 0.2‖ | 1.8 ± 1.1 |
| Boundary¶ | 36.2 ± 0.6 | 47.6 ± 4.1‖ | 151.1 ± 17.4‖ |

* In Na-Ringer's at 15°C with 5 μM labeled ouabain (60 μCi/ml) followed by 30-min wash.

‡ Mean ± SE ($n$ = 13 sections of freeze-dried slice representing two fish); combined 1- and 4-h data from Table III with inclusion of boundary data.‡

§ Mean ± SE above background density ($n$ = 13 and 3 sections representing two and one fish, respectively, for 1- and 4-h incubation). Autoradiographic exposure times ranged from 3 to 17 d.

‖ Significantly ($P < 0.05$) different from background density.

¶ Central membrane and central mitochondrial regions exclusive of the 1-μm wide, membrane-mitochondrial boundary region (Fig. 13).

Autoradiographic grain counting provides a means for quantitating the bound ouabain in individual regions of the rectal gland epithelium. As shown in Table IV, mean grain densities for all but the membrane-mitochondrial boundary are low and, in fact, not always significantly ($P < 0.05$) above background density. Generally, ouabain does not reach intracellular organelles and, predictably, the lowest densities are associated with the nuclear and central mitochondrial regions. More interesting is the apical region, which, in spite of its small area, includes the cell surface bordering the tubular lumen and, hence, represents a possible locus for binding. Because, however, ouabain exposure was almost certainly adequate in thin slices with open lumens, the relatively low densities after both 1- and 4-h incubations indicate, at most, minor apical binding. In contrast, the major locus of binding appears to be the membrane-mitochondrial boundary region over which were located 80 and 87% of the total grains, respectively, after 1 and 4 h of incubation (computed from area and density data in Table IV). The possibility of delayed ouabain movement from incubation medium into the central membrane region is effectively ruled out by the 4-h density values which, for the central region, remained low but, for the boundary region, more than doubled (Table IV). Thus, the only autoradiographic density data that parallel the actual slice data for bound ouabain (Fig. 3) are those for the boundary region.

Finally, steady-state values for bound ouabain in picomoles per milligram tissue were derived using the autoradiographic conversion factor obtained with [$^3$H]ouabain standards and the grain densities for the membrane-mitochondrial boundary region (Table IV). Taking the 4-h mean to represent the steady state and doubling the 1-h mean (half-loading time approximates 1 h), a weighted mean for the steady state density was calculated to be 106 grains/1,000 $\mu m^2$ per $d$ ($n$ = 16 sections). This steady-state grain density converts to 116 pmol ouabain/mg boundary region. Further correction for the relative cell area (36%) and the fact that epithelial cells comprise only part of the rectal gland slice (75% estimated for incubated slices in which the connective tissue matrix is somewhat swollen) leads to 31 pmol ouabain/mg slice. Considering ±25% accuracy for present [$^3$H]ouabain autoradiography, this steady-state value agrees well with the actual slice data which approaches ~25 pmol/mg tissue (Figs. 3 and 4). Such agreement further strengthens the evidence for the primary locus of ouabain binding being in the boundary region, because the present autoradiographs were clearly produced by a full complement of [$^3$H]ouabain-filled sites, i.e., no differential loss or leaching occurred from the central membrane region during tissue processing. Actually, for present slices incubated in 5 $\mu$M ouabain, which approximates Ki, half of the total or maximal number of binding states should be filled at steady state. Thus, by doubling the autoradiographic values given above, maximal steady-state binding was estimated as 60 and 230 pmol ouabain/mg, respectively, of rectal gland slice and of membrane-mitochondrial boundary region. Interestingly, this boundary region maximum for rectal gland cells is essentially identical to a corresponding binding value for gill Cl cells from seawater-adapted killifish (16), 240 pmol ouabain/mg of tubular system region. Both tissues contain large amounts of basal-lateral membrane in close proximity to mitochondria.

## DISCUSSION

The present study with incubated slices of dogfish rectal gland clearly establishes that most of the enormous Na,K-ATPase activity associated with the tubular cells is located at the basal and lateral cell surface facing interstitial fluid, not at the luminal surface facing secreted fluid. Moreover, the distribution of Na,K-ATPase along the highly infolded basal-lateral membrane appears to be nonuniform, with the highest density of enzyme sites close to the mitochondria, i.e., at the membrane-mitochondrial boundary. These conclusions are based on several lines of evidence. First, characterization experiments with ouabain demonstrated high-affinity binding which correlated with Na,K-ATPase inhibition and half-saturation at 5 $\mu$M ouabain. At this concentration, the normal half-loading time was ~1 h. Thus, convincing Na,K-ATPase localization should be provided by present 1- and 4-h autoradiographs which reflect specific [$^3$H]ouabain binding by up to half of the functional enzyme sites. This claim is confirmed by the quantitative agreement between slice and autoradiographic data for bound ouabain. Second, comparison with aldehyde-fixed morphology indicated that rapid freezing followed by freeze drying did not grossly alter the primary cell regions in slices used for autoradiography. In particular, electron micrographs showed that the infoldings of basal-lateral membrane were neither displaced

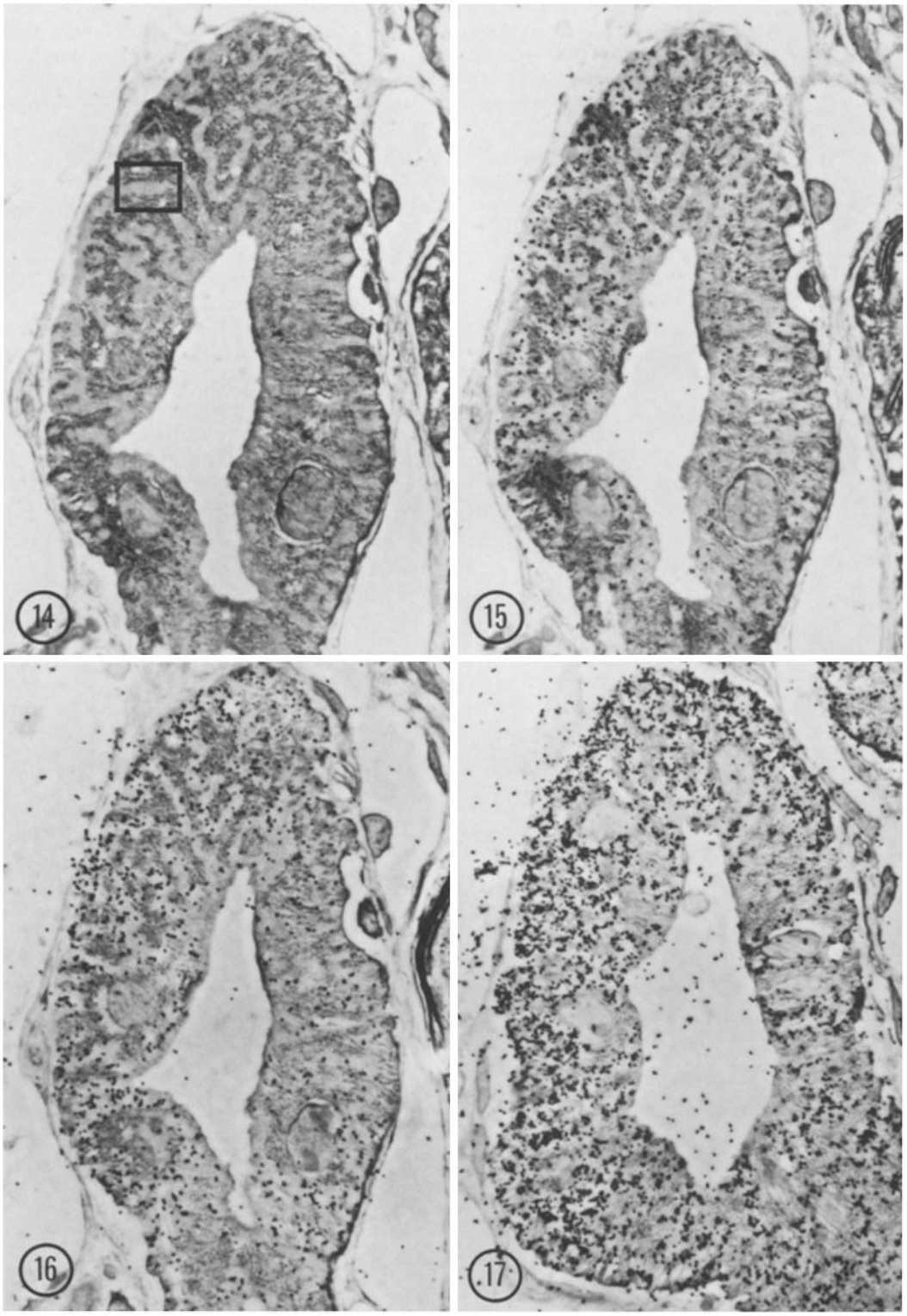
14
15
16
17

from the central membrane region nor concentrated at the membrane-mitochondrial boundary. Thus, the high density of Na,K-ATPase observed in the boundary compared to the central membrane region cannot be attributed to a freezing artifact in present [$^3$H]ouabain autoradiographs. Third, this nonuniform distribution of Na,K-ATPase sites was observed in 4-h autoradiographs with essentially steady-state binding of [$^3$H]ouabain. In fact, at both 1 and 4 h the boundary region contained ~85% of the labeled sites in rectal gland cells. Thus, low site density in the central membrane region is not an artifact resulting from slow entry into the extracellular fluid channels of this region. Fourth, one of the characteristics of cell surface or plasma membranes is the presence of Na,K-ATPase. In contrast, this enzyme is not generally present in mitochondria nor does ouabain generally penetrate cell surfaces (15, 27). Thus, we conclude that the high density of enzyme sites in the membrane-mitochondrial boundary represents Na,K-ATPase located in the folds of the basal-lateral cell membranes which are in close apposition to the mitochondria.

The only previous report on Na,K-ATPase localization in the elasmobranch rectal gland is a cytochemical study by Goertemiller and Ellis (14) using Sr-capture Pb-substitution cytochemistry. The criteria for measurement of *p*-nitrophenyl phosphatase were established in the now classic work of Ernst (8, 9) and Ernst and Philpott (11) who developed the method using avian nasal gland slices. The method is based on the K-dependent *p*-nitrophenyl phosphatase activity of Na,K-ATPase, and Ernst (8) systematically adjusted conditions so that final nasal gland slices retained almost 20% of this activity. By using essentially the same conditions without further adjustment as Goertemiller and Ellis (14) we calculated that rectal gland slices retained only 0.02% enzyme activity by a conservative estimate.[1] This remaining enzyme activity may clearly be too low for its localization to be representative of the localization of the total enzyme population. Thus, we believe that the seemingly uniform distribution of reaction product found along the basal-lateral membranes by Goertemiller and Ellis (14) should not be considered a serious contradiction of the nonuniform

[1] Goertemiller and Ellis reported rectal gland slice K-dependent, ouabain-sensitive nitrophenyl phosphatase (NPPase) activity as 0.0706 μmol of nitrophenyl phosphate (NPP) released/g of tissue/h (0.0850 in standard medium minus 0.0144 in K-free medium containing $10^{-3}$ M ouabain). Assuming a protein conversion of 10%, or 100 mg protein/g tissue, their value is 0.000706 μmol NPP/mg protein per h. If one assumes that the transport enzyme hydrolyzes NPP at 1/10th the rate at which it hydrolyzes ATP (see reference 14 for pertinent literature), then their NPPase value converts to a Na,K-ATPase value of 0.00706 μmol $P_i$/mg protein per h, or 0.02% of the enzyme activity (39.4 μmol $P_i$/mg protein per h) reported by us in the present study.

FIGURE 14 Ouabain-incubated tubule after freezing and freeze drying. Seen in slightly oblique section, the morphological appearance at the light microscope level is remarkable similar to that of comparable tubules with aldehyde fixation (Figs. 7 and 8). The only obvious freezing artifacts are some shrinkage of cell nuclei, as evidenced by open clefts (unstained), and extensive condensation of individual mitochondria, as evidenced by the punctate appearance of mitochondrial clusters (dark stained). More important, the boundary between mitochondrial clusters and basal-lateral membranes (light stained) is clearly identifiable, e.g., in area (black rectangle) oriented as the schema in Fig. 13. Tubules from deeper within incubated slices, where freezing was slower, exhibited greater cryosmotic distortion (Fig. 18) and were excluded from study. The present tubule was at the edge of the incubated slice, as evidenced by the closely applied strip of rectal gland capsule (left side). The slice was incubated 1 h at 15°C in Na-Ringer's containing 5 μM [$^3$H]ouabain, washed 30 min, rapidly frozen, freeze dried, and plastic embedded before sectioning. Most of the 1-μm plastic sections were coated with emulsion for autoradiographs (Figs. 15–17); the present uncoated section was stained lightly and photographed with phase-contrast optics. × 1,000.

FIGURES 15–17 [$^3$H]Ouabain autoradiographs of a 1-h incubated tubule exposed for 3, 9, and 33 d, respectively. The developed silver grains (black dots) in the emulsion coat overlying the tissue section increase in number with autoradiographic exposure time. At a given exposure, the grain density corresponds to the tissue content of bound ouabain (see text). Although not strictly serial, the sections show the same tubule as in Fig. 14. Slice incubation and section preparation as for Fig. 14; 1-μm sections coated with 2-μm autoradiographic emulsion, developed on completion of exposure, stained lightly, and photographed with phase-contrast optics focused to show grains superimposed over tissue. × 1,000.

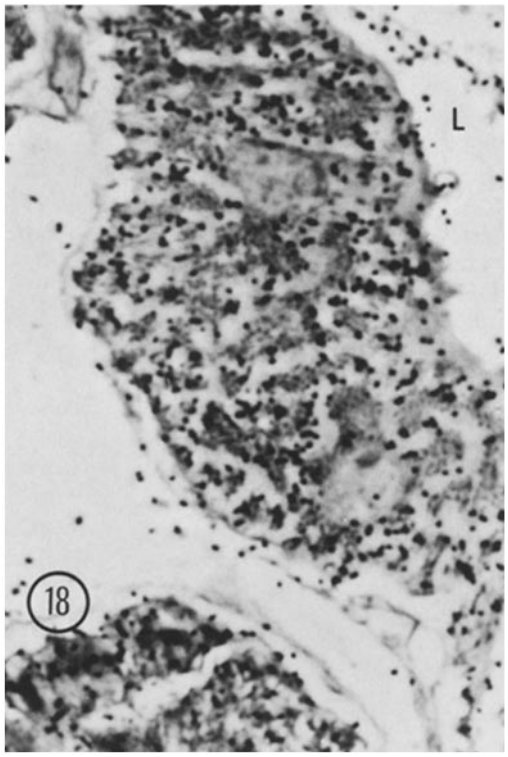


FIGURE 18 [$^3$H]Ouabain autoradiography of 4-h incubated tubular epithelium exposed 4 d. Freeze-dried morphology is good in the tubule with part of the lumen (*L*) showing; cryosmotic distortion is more pronounced in the portion of a deeper tubule. Rectal gland slice from a second dogfish incubated long enough for ouabain binding to approach steady state; otherwise, autoradiograph prepared and photographed as in Figs. 15–17. × 1,600.

Na,K-ATPase distribution indicated in the present [$^3$H]ouabain autoradiographs. We are aware of only one other epithelium, that of the frog gallbladder, where [$^3$H]ouabain autoradiography has shown nonuniform distribution of Na,K-ATPase (20). Mills and DiBona showed that in this epithelium twice as much ouabain was bound at the basal end of the epithelial cells as at the apical end. They attributed this difference to membrane amplification in the basal end of the cell, and so, in fact, the ouabain binding may be uniform with respect to membrane surface area. However, this explanation does not appear to be valid for the rectal gland.

It is of especial interest that the Na,K-ATPase sites in rectal gland cells are localized to the basal-lateral membranes in direct juxtaposition to the mitochondria and, accordingly, in close proximity to the energy source for pumping the Na out of the cell into the interstitial fluid. The basal-lateral localization initially appeared as paradoxical, because the function of the elasmobranch rectal gland is to secrete a hyperosmolar NaCl solution into the tubular lumen to maintain homeostasis. Thus, the pump appears to be oriented in the wrong direction for removing Na from the organism and in direct opposition to the known direction of NaCl transport. This apparent paradox extends to many other osmoregulatory organs, whose salt-secreting cells likewise possess an enormously amplified basal-lateral membrane surface, such as the teleost fish gill (16), the iguana and marine turtle salt glands (5, 6), the avian salt gland (9, 10, 18), and the human sweat gland (24). It has been suggested that the primary role of the basal-lateral Na,K-ATPase is merely the regulation of intracellular ion content and cell volume (23), activities required for the normal metabolic activity of all vertebrate cells. Yet the extremely high activity of Na,K-ATPase in the rectal gland of the dogfish implies a function for the enzyme that extends beyond that of maintaining normal intracellular ionic compositions.

Studies on the isolated, perfused rectal gland (29, 30, 35) indicate that Cl is actively secreted across the tubule cell against an electrical and chemical gradient. Secretion of Cl is inhibited by ouabain, presumably through the inhibition of Na,K-ATPase. A tentative hypothesis for Cl secretion has been formulated (30) in which the uphill transport of Cl into the cell is coupled through a membrane carrier with the downhill movement of Na into the cell along its electrochemical gradient. The gradients impelling the movement of Na into the cell are maintained by the Na,K-ATPase pump located in the basal-lateral membranes. Cl within the cell would be extruded into the lumen by negative intracellular electrical forces, and Na in the lateral intercellular spaces would diffuse down its electrical gradient directly across the junctional complexes into the tubular lumen. The function of the Na,K-ATPase in this schema is to maintain a low intracellular Na concentration, thus facilitating the passive entry of Na into the cell with the concomitant coupled transfer of Cl. Cl secretion can thus be regarded as an example of secondary active transport depending indirectly upon Na,K-ATPase.

An important feature of this hypothesis is that

the location of the Na,K-ATPase does not determine the direction of transepithelial secretion, which depends rather on the relative location and activity of coupled Na-Cl carriers and on the relative permeabilities of the mucosal and serosal faces of the cell to Cl. The basal-lateral localization of the enzyme, demonstrated in the present study, is entirely consistent with this model. Direct evidence has recently been adduced in favor of this hypothesis by the demonstration of coupled Na-Cl transport in plasma membrane vesicles isolated from the rectal gland of *S. acanthias* (12).

An alternative theory to explain the basal-lateral orientation of Na,K-ATPase in the avian salt gland was recently advanced by Ellis et al. (7). They postulated that the function of the enzyme was to concentrate NaCl in the intercellular channels in a standing gradient responsible for the passive reabsorption of water from a progressively concentrated luminal solution. This schema would not apply to the elasmobranch rectal gland, which secretes a fluid isotonic with plasma and high in NaCl by virtue of being low in urea. Nor would it account for the negative luminal electrical potential observed in the rectal gland which, together with the ionic gradient opposing Cl secretion, argues strongly for the active transport of Cl (30).

The rectal gland resembles many other organs such as the teleost gill, avian salt gland, cornea, intestine, mammary gland, and human sweat gland in its possession of extensive basal-lateral membranes, rich in Na,K-ATPase, and oriented so as to pump Na in a direction opposite to the direction of net secretion of electrolytes. It seems likely that the primary mechanism for such secretion is the secondary active transport of Cl, dependent for its ultimate source of energy on the hydrolysis of ATP by the basolateral Na,K-ATPase.

The authors thank Mr. Harold Church, Ms. Kate Spokes, and Ms. Susan Burnham for their excellent technical assistance.

This investigation was supported by United States Public Health Service grants AM15973 (Dr. Kinter), AM18078 (Dr. Epstein), GM57244 and GM 24766 (Dr. Karnaky), RR05764 (Mount Desert Island Biological Laboratory), and RR05417 (Temple University Medical School), and by National Science Foundation grant PCM75-03098A02 (Mount Desert Island Biological Laboratory). Dr. Silva is an Established Investigator of the American Heart Association.

Preliminary aspects of this study appeared in Karnaky, K. J., Jr., P. Silva, and W. B. Kinter. 1976. *Bull. Mt. Desert Isl. Biol. Lab.* **16**:64–65.

*Received for publication 1 September 1978, and in revised form 14 May 1979.*

## REFERENCES

1. Bonting, S. L. 1970. Sodium-potassium-activated adenosinetriphosphatase and cation transport. *In* Membranes and Ion Transport. Vol. 1. E. E. Bittar, editor. John Wiley & Sons, Inc., New York. 257–363.
2. Bulger, R. E. 1963. Fine structure of the rectal (salt-secreting) gland of the spiny dogfish, *Squalus acanthias*. *Anat. Rec.* **147**:95–127.
3. Burger, J. W., and W. N. Hess. 1960. Function of the rectal gland in the spiny dogfish. *Science (Wash. D.C.).* **131**:670–671.
4. Clausen, T., and O. Hansen. 1977. Active Na-K transport and the rate of ouabain binding. The effect of insulin and other stimuli on skeletal muscle and adipocytes. *J. Physiol. (Lond.).* **270**:415–430.
5. Ellis, R. A., and C. C. Goertemiller, Jr. 1974. Cytological effects of salt-stress and localization of transport adenosine triphosphatase in the lateral nasal glands of the desert iguana, *Dipsosaurus dorsalis*. *Anat. Rec.* **180**:285–298.
6. Ellis, R. A., and C. C. Goertemiller, Jr. 1976. Scanning electron microscopy of intercellular channels and the localization of ouabain sensitive *p*-nitrophenyl phosphatase activity in the salt-secreting lacrymal glands of the marine turtle, *Chelonia mydas*. *Cytobiologie.* **13**:1–12.
7. Ellis, R. A., C. C. Goertemiller, Jr., and D. L. Stetson. 1977. Significance of extensive 'leaky' cell junctions in the avian salt gland. *Nature (Lond.).* **268**:555–556.
8. Ernst, S. A. 1972. Transport adenosine triphosphatase cytochemistry. I. Biochemical characterization of a cytochemical medium for the ultrastructural localization of ouabain-sensitive, potassium-dependent phosphatase activity in the avian salt gland. *J. Histochem. Cytochem.* **20**:13–22.
9. Ernst, S. A. 1972. Transport adenosine triphosphatase cytochemistry. II. Cytochemical localization of ouabain-sensitive, potassium-dependent phosphatase activity in the secretory epithelium of the avian salt gland. *J. Histochem. Cytochem.* **20**:23–38.
10. Ernst, S. A., and J. W. Mills. 1977. Basolateral plasma membrane localization of ouabain-sensitive sodium transport sites in the secretory epithelium of the avian salt gland. *J. Cell Biol.* **75**:74–94.
11. Ernst, S. A., and C. W. Philpott. 1970. Preservation of the $Na^+$-$K^+$-activated and $Mg^+$-activated adenosine triphosphatase activities of avian salt gland and teleost gill with formaldehyde as fixative. *J. Histochem. Cytochem.* **18**:251–263.
12. Eveloff, J., R. Kinne, E. Kinne-Saffran, H. Murer, J. S. Stoff, P. Silva, F. H. Epstein, and W. B. Kinter. 1978. Coupled Na/Cl transport into plasma membrane vesicles from dogfish rectal gland. *Fed. Proc.* **37**:625.
13. Forrest, J. N., Jr., A. D. Cohen, D. A. Schon, and F. H. Epstein. 1973. Na transport and Na-K-ATPase in gills during adaptation to seawater: effects of cortisol. *Am. J. Physiol.* **224**:709–713.
14. Goertemiller, C. C., Jr., and R. A. Ellis. 1976. Localization of ouabain-sensitive, potassium-dependent nitrophenyl phosphatase in the rectal gland of the spiny dogfish, *Squalus acanthias*. *Cell Tiss. Res.* **175**:101–112.
15. Hokin, L. E. 1978. Reconstitution of the $Na^+$-$K^+$ pump from the purified ($Na^+ + K^+$)-activated adenosine triphosphatase from the rectal gland of *Squalus acanthias*. *In* Membrane Transport Processes. Vol. 2. D. C. Tosteson, Y. A. Ovchinnikov, and R. Latorre, editors. Raven Press, New York. 399–416.
16. Karnaky, K. J., Jr., L. B. Kinter, W. B. Kinter, and C. E. Stirling. 1976. Teleost chloride cell. II. Autoradiographic localization of gill Na,K-ATPase in killifish *Fundulus heteroclitus* adapted to low and high salinity environments. *J. Cell Biol.* **70**:157–177.
17. Maetz, J., and M. Bornancin. 1975. Biochemical and biophysical aspects of salt excretion by chloride cells in teleosts. *Fortschr. Zool.* **23**(2/3):322–362.
18. Mazurkiewicz, J. E., and R. J. Barrnett. 1978. Immunocytochemical localization of Na,K-ATPase in the secretory epithelium of the avian salt gland. *J. Cell Biol.* **79**(2, ft. 2):216a. (Abstr.).
19. Meryman, H. T. Review of biological freezing. *In* Cryobiology. H. T. Meryman, editor. Academic Press, New York. 1–114.
20. Mills, J. W., and D. R. Dibona. 1978. Distribution of $Na^+$ pump sites in the frog gall bladder. *Nature (Lond.).* **271**:273–275.
21. Mills, J. W., and S. A. Ernst. 1975. Localization of sodium pump sites in the frog urinary bladder. *Biochim. Biophys. Acta.* **375**:268–273.
22. Mills, J. W., S. A. Ernst, and D. R. Dibona. 1977. Localization of

Na-pump sites in the frog skin. *J. Cell Biol.* **73**:88–110.
23. PEAKER, M., and J. LINZELL. 1975. Salt Glands in Birds and Reptiles. Cambridge University Press, Cambridge, England. 86–111.
24. QUINTON, P. M., and J. McD. TORMEY. 1973. Localization of Na/K-ATPase sites in the secretory and reabsorptive epithelia of perfused eccrine sweat glands: a question to the role of the enzyme in secretion. *J. Membr. Biol.* **29**:383–399.
25. QUINTON, P. M., E. M. WRIGHT, and J. McD. TORMEY. 1973. Localization of sodium pumps in the choroid plexus epithelium. *J. Cell Biol.* **58**:724–730.
26. RENFRO, J. L., D. S. MILLER, K. J. KARNAKY, JR., and W. B. KINTER. 1976. Na,K-ATPase localization in teleost urinary bladder by [$^3$H]-ouabain autoradiography. *Am. J. Physiol.* **231**:1735–1743.
27. SCHWARTZ, A., G. E. LINDENMAYER, and J. C. ALLEN. 1975. The sodium-potassium adenosine triphosphatase: pharmacological, physiological and biochemical aspects. *Pharmacol. Rev.* **27**:1–134.
28. SHAVER, J. L., and C. STIRLING. 1978. Ouabain binding to renal tubules in the rabbit. *J. Cell Biol.* **76**:278–292.
29. SIEGEL, N. J., D. A. SCHON, and J. P. HAYSLETT. 1976. Evidence for active chloride transport in dogfish rectal gland. *Am. J. Physiol.* **230**: 1250–1254.
30. SILVA, P., J. STOFF, M. FIELD, L. FINE, J. N. FORREST, and F. H. EPSTEIN. 1977. Mechanism of active chloride secretion by shark rectal gland: role of Na-K-ATPase in chloride transport. *Am. J. Physiol.* **233**: F298–F306.
31. STIRLING, C. E. 1972. Radioautographic localization of sodium pump sites in rabbit intestine. *J. Cell Biol.* **53**:704–714.
32. STIRLING, C. E. 1976. High-resolution autoradiography of [$^3$H]ouabain binding in salt transporting epithelia. *J. Microsc. (Oxf.).* **106**(2):145–157.
33. STIRLING, C. E., and W. B. KINTER. 1967. High resolution autoradiography of galactose-$^3$H accumulation in rings of hamster intestine. *J. Cell Biol.* **35**:585–604.
34. STIRLING, C. E., A. J. SCHNEIDER, M.-D. WONG, and W. B. KINTER. 1972. Quantitative autoradiography of sugar transport in intestinal biopsies from normal humans and a patient with glucose-galactose malabsorption. *J. Clin. Invest.* **51**:438–451.
35. STOFF, J. S., P. SILVA, M. FIELD, J. FORREST, A. STEVENS, and F. H. EPSTEIN. 1977. Cyclic AMP regulation of active chloride transport in the rectal gland of marine elasmobranchs. *J. Exp. Zool.* **199**:443–448.